

PAPER

Inactivation of *Candida albicans* biofilms by atmospheric gliding arc plasma jet: effect of gas chemistry/flow and plasma pulsing

To cite this article: A C O C Doria *et al* 2019 *Plasma Res. Express* **1** 015001

View the [article online](#) for updates and enhancements.

You may also like

- [The Discovery of a Potential Antimicrobial Agent: the Novel Compound Natural Medicinal Plant Fermentation Extracts against *Candida albicans*](#)
Mingzhu Song, Xirui Wang, Canquan Mao et al.
- [Discharge and jet characteristics of gliding arc plasma igniter driven by pressure difference](#)
Xinyao CHENG, , Huimin SONG et al.
- [Antifungal activity of biosynthesized silver nanoparticles from *Candida albicans* on the strain lacking the *CNP41* gene](#)
Darshan Dhabalia, Shareefraza J Ukkund, Usman Taqui Syed et al.

HIDEN ANALYTICAL

Analysis Solutions for your Plasma Research

- Knowledge
- Experience ■ Expertise

[Click to view our product catalogue](#)

Contact Hiden Analytical for further details:

- W www.HidenAnalytical.com
- E info@hiden.co.uk

Surface Science

- ▶ Surface Analysis
- ▶ SIMS
- ▶ 3D depth Profiling
- ▶ Nanometre depth resolution

Plasma Diagnostics

- ▶ Plasma characterisation
- ▶ Customised systems to suit plasma Configuration
- ▶ Mass and energy analysis of plasma ions
- ▶ Characterisation of neutrals and radicals

Plasma Research Express



PAPER

Inactivation of *Candida albicans* biofilms by atmospheric gliding arc plasma jet: effect of gas chemistry/flow and plasma pulsing

A C O C Doria¹, F R Figueira¹, J S B de Lima², J A N Figueira³, A H R Castro⁴, B N Sismanoglu⁴, G Petraconi⁴, H S Maciel^{2,4}, S Khouri⁵ and R S Pessoa^{1,2,4,6} 

¹ Laboratório de Biotecnologia e Plasmas Elétricos, IP&D, Universidade do Vale do Paraíba, Av. Shishima Hifumi 2911, 12244-000, São José dos Campos, SP, Brazil

² Instituto Científico e Tecnológico, Universidade Brasil, Rua Carolina Fonseca 235, 08230-030, São Paulo, SP, Brazil

³ Divisão de Engenharia Mecânica, Instituto Tecnológico de Aeronáutica, Praça Marechal Eduardo Gomes 50, 12228-900, São José dos Campos, SP, Brazil

⁴ Centro de Ciência e Tecnologia de Plasmas e Materiais—PlasMat, Instituto Tecnológico de Aeronáutica, Praça Marechal Eduardo Gomes 50, 12228-900, São José dos Campos, SP, Brazil

⁵ Núcleo de Estudos Farmacêuticos e Biomédicos da Faculdade de Ciências da Saúde, Universidade do Vale do Paraíba, Av. Shishima Hifumi 2911, 12244-000, São José dos Campos, SP, Brazil

⁶ Author to whom any correspondence should be addressed.

E-mail: rspessoa@ita.br

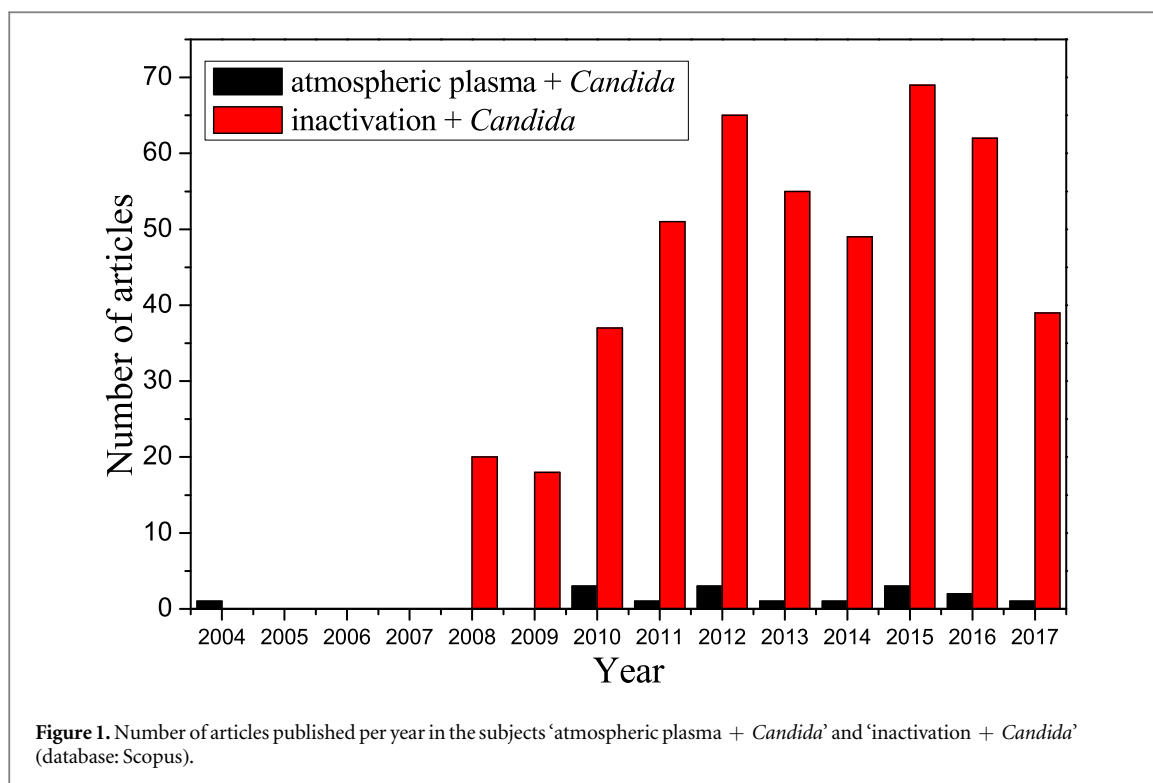
Keywords: *Candida albicans*, biofilm, atmospheric plasma, gliding arc discharge, FT-IR, SEM, optical emission spectroscopy

Abstract

Candida spp are present in 70%–90% of invasive infections and non-thermal plasmas operated at atmospheric pressure have been gaining attention as a new antimicrobial strategy for medical devices. This work presents studies on the inactivation efficacy of biofilms of *Candida albicans* grown in polyurethane (PU), main constituent of central venous catheter, by atmospheric gliding arc plasma jet operated at different process parameters: gas chemistry/flow (argon, helium, or its mixture with air) and plasma pulsing. The investigation was performed in the post-discharge region of the plasma jet. After plasma treatment, the colony-forming units (CFU) were counted, and the chemical bonding (FT-IR) and morphological (SEM) analyses of the surface of the biofilm plus PU substrate were investigated. Furthermore, optical emission spectroscopy (OES) technique was applied to characterize the plasma chemistry and measure the OH concentration and rotational temperature, together with thermal analyses of the substrate during treatment. CFU results showed that gliding arc plasma jet was efficient for the inactivation of *C. albicans* biofilms. It obtained a maximum CFU reduction of 100% and 98% for 4 L min⁻¹ air/6 L min⁻¹ He and 99% and 98% for 4 L min⁻¹ air/6 L min⁻¹ Ar in continuous and pulsed mode, respectively. SEM and FT-IR analyses corroborate with results of % CFU reduction, showing a reduction of the biofilm constituents on the substrate surface. From OES and substrate thermal analyses, it was possible to verify that, although the OH concentration and rotational temperature of air/He plasma jet are lower in comparison to the air/Ar, a drastic increase of the substrate temperature during the treatment (up to 70 °C) was observed for this plasma chemistry.

1. Introduction

The *Candida albicans*, a commensal yeast of the human microbiota, is one of the most significant causes of nosocomial infections of fungal origin [1–3]. Systemic infection by *C. albicans* shows a mortality rate of 30%–50%, being the immunocompromised patients more susceptible [1]. Infections begin with the adhesion of microorganisms to invasive medical devices and implants, initiating the formation of treatment-resistant biofilms [1]. These biofilms consist of microorganisms adhered to a surface associated with extracellular matrix polymers, being therefore more resistant to antibiotics and to immunological factors when compared to planktonic cells [4]. The prevention of the formation of biofilms needs to be focused on two main aspects: (a) control of the presence of microorganisms in the environment and (b) creation of new products with surfaces



or conditions that hinder the primary adhesion of microorganisms [5–7]. In the case of contamination, sterilization processes using physical and chemical methods have been adopted for the complete destruction of microorganisms [5–9]. All traditional methods show efficacy when applied to free-living microorganisms, but are not as effective when applied to biofilm [5]. Therefore, the study of new technologies for the control of microbial contamination becomes important due to the number of deaths caused by nosocomial infections each year, as well as the environmental problems caused by the large amount of hospital waste that can be reprocessed through a safe, inexpensive and environment clean technique. In this scope, the plasma technology for the sterilization process is growing and gaining attention.

Atmospheric plasmas have shown great potential in many applications in the biomedical and dental fields, such as induction of apoptosis in cancer cells, wound sterilization and surgical instruments [10]. Another current application is the sterilization of heat-sensitive medical devices such as catheters and endoscopes [11, 12]. In this field of research, promising results on the efficacy of non-thermal plasmas in microbial inactivation have been demonstrated for microorganisms in the form of biofilm or planktonic cells from bacteria, fungi, viruses and spores [13–15]. It is believed that the effectiveness is due to plasma derived products, such as reactive oxygen species (ROS), reactive nitrogen species (RNS), UV radiation and charged particles [13, 16, 17]. The exact mechanism of inactivation is not well elucidated; hypotheses converge to the presence of ROS and RNS, which play an important role in the vital physiological processes of microorganisms. At low doses, reactive species act to promote cell survival, proliferation and migration. At high doses, they cause oxidative stress related to cellular aging, initiation and execution of apoptosis [13].

There are several geometries that generate non-thermal plasmas at atmospheric pressure, such as corona discharge, dielectric barrier discharge (DBD), micro plasmas and plasma jets. Among the discharges geometries for generating plasma jets, we can mention the gliding arc (GA) discharge. It is a self-oscillating discharge that starts between the electrodes of divergent geometry; through the force of the laminar or turbulent flow, is elongated and cooled until it is extinguished. At the same time, a new discharge arc is created in the smallest gap between the electrodes [18]. The GA operates at atmospheric or higher pressure and the power dissipated under non-equilibrium conditions can reach values of the order of tens of W to kW per pair of electrodes. The advantage compared to other devices is the low cost and simplicity of construction [10, 13].

The number of studies on the application of plasma in microorganisms of the genus *Candida* has emerged in the last decade, mainly due to the clinical importance of this fungus. Figure 1 shows the distribution of articles published per year in the themes 'atmospheric plasma + *Candida*' and 'inactivation + *Candida*'. Among these studies, Wang *et al* tested the application of a plasma jet as an alternative to the resistance of biofilms to drugs using an Ar and O₂ plasma jet in biofilm of *C. albicans* formed on the base of resin denture [17]. The results showed that ~100 μm thick biofilms were completely inactivated after 8 min of treatment. Rahimi-Verki *et al* studied the effect of cold plasma on the growth of *C. albicans* with emphasis on biofilm formation, ergosterol

formation, activities and phospholipid secretion of proteinase enzymes, which are virulence factors of the fungus [19]. The plasma used was He/O₂ (2%) with irradiation times of 90, 120, 150, and 180 s. Their results showed a reduction of growth from 31% to 82%, based on the determined exposure times. The ergosterol biosynthesis was exhibited between 41% to 91%; and biofilm formation was reduced from 43% to 57%. The activities of the phospholipid and proteinase enzyme were reduced from 4% to 45%. Recently, Borges *et al* analyzed the effects of cold atmospheric pressure plasma jet operated with Helium (He-CAPPJ) on *C. albicans* virulence traits and biofilms [20]. They concluded that He-CAPPJ was able to attenuate fungal adhesion and morphogenesis with low cytotoxicity after short periods of treatment. Effective exposure periods against biofilms were cytotoxic to Vero cells. He-CAPPJ did not present genotoxic effect. In another recent study, Simomura *et al* evaluated the influence of exposure time to argon/water vapor GA plasma jet on surface sterilization of a *C. albicans* contaminated silicone substrate [21]. The results indicated a CFU reduction of up to 97.5% for treatment time of 20 min.

In a recent study, Doria *et al* have demonstrated that the treatment of biofilms of *C. albicans* in the post-discharge region of an atmospheric GA plasma jet is an interesting alternative for the treatment of surfaces contaminated by microorganisms [22]. Basically, the effect of air insertion on the argon GA discharge has been investigated, and further investigations are required. This work presents studies on the inactivation efficacy of *C. albicans* biofilms, grown *in vitro*, on polyurethane (PU) substrate by atmospheric plasma jets operated in different process parameters: gas chemistry (argon, helium, or its mixture with air) and flow, and plasma operation in continuous or pulsed mode. The motivation for the use of the PU substrate is its application as the main constituent of the central venous catheter, whose traditional methods of sterilization cannot be used and, therefore, this type of biomedical device is discarded.

2. Materials and methods

2.1. Microorganisms preparation

The preparation of the fungal suspensions of a standard strain of *C. albicans* ATCC 10231 (ATCC is American Type Culture Collection, Manassas, VA, USA) was performed *in vitro* with the Sabouraud Dextrose broth (DIFCO) at a concentration compatible with 0.5 in MacFarland turbidity scale (10⁶ CFU/mL). The strains were kept frozen at -20 °C in glycerol, subsequently peaked in Sabouraud, and incubated at 37 °C in an oven for 48 h before being used in experiments, respecting all biosafety standards.

2.2. Biofilm growth and samples group

Polyurethane plates (3 R Plásticos, São Paulo, SP, Brazil) of 2 mm thickness and 1 cm² area were used as substrates. These plates were washed with a multienzyme detergent and dried. Subsequently, the PU plates were placed in vials containing 20 ml of the previously prepared fungal suspension and incubated at 37 °C for 48 h under constant stirring at 110 rpm in an incubator shaker (Marconi MA 420, Piracicaba, SP, Brazil). After the first 24 h of incubation, the culture medium was replaced for maintenance of the nutrients required for fungal growth. At the end of the incubation period, the samples were removed from the vials and transferred to new bottles which contained phosphate buffer solution (PBS pH 7.2 ± 0.1) to remove non-adhered cells and preserve the integrity of the biofilm on the surface of the substrate [22].

2.3. Experimental setup

The experimental system setup included: the plasma reactor, the high-voltage power supply, the pulsing circuit, the oscilloscope, and the optical emission spectrometer (figure 2). The GA plasma was generated in a forward vortex flow reactor (FVFR) type [18] and this is composed of plasma jet and post-discharge regions. The gases used in this study were argon (purity of 99.95%), helium (purity of 99.5%) and dry air generated by medical/orthodontic compressor (Schulz MSV6-30, Joinville, SC, Brazil). The gases were inserted into FVFR with a total flow rate of 10 L min⁻¹ using separated rotameters. To generate the plasma, a high-voltage transformer (7.5 kV, 60 Hz) was connected to the electrodes. A high-voltage resistance (1 kΩ) protects the transformer in the event of electric arc. A Variac transformer (VARIAC, Cleveland, OH, USA) was used to control the electrical voltage. The applied voltage and current signals were measured with a numerical oscilloscope (Tektronix TDS2024B; Tektronix, Beaverton, OR) with a high-voltage probe (Tektronix P6015A) and a self-adjustable probe (Agilent N2869B). For the case of current signal, this was inferred from shunt resistor in series with grounded electrode. In addition, it is important to note that as plasma plume goes out from the nozzle, this means that a flux of charged particles escapes the supply system circuit. Therefore, a part of the current cannot be measured by the evaluation of the current flowing in the supply circuit, which consequently increases the error in the measurement of discharge power.

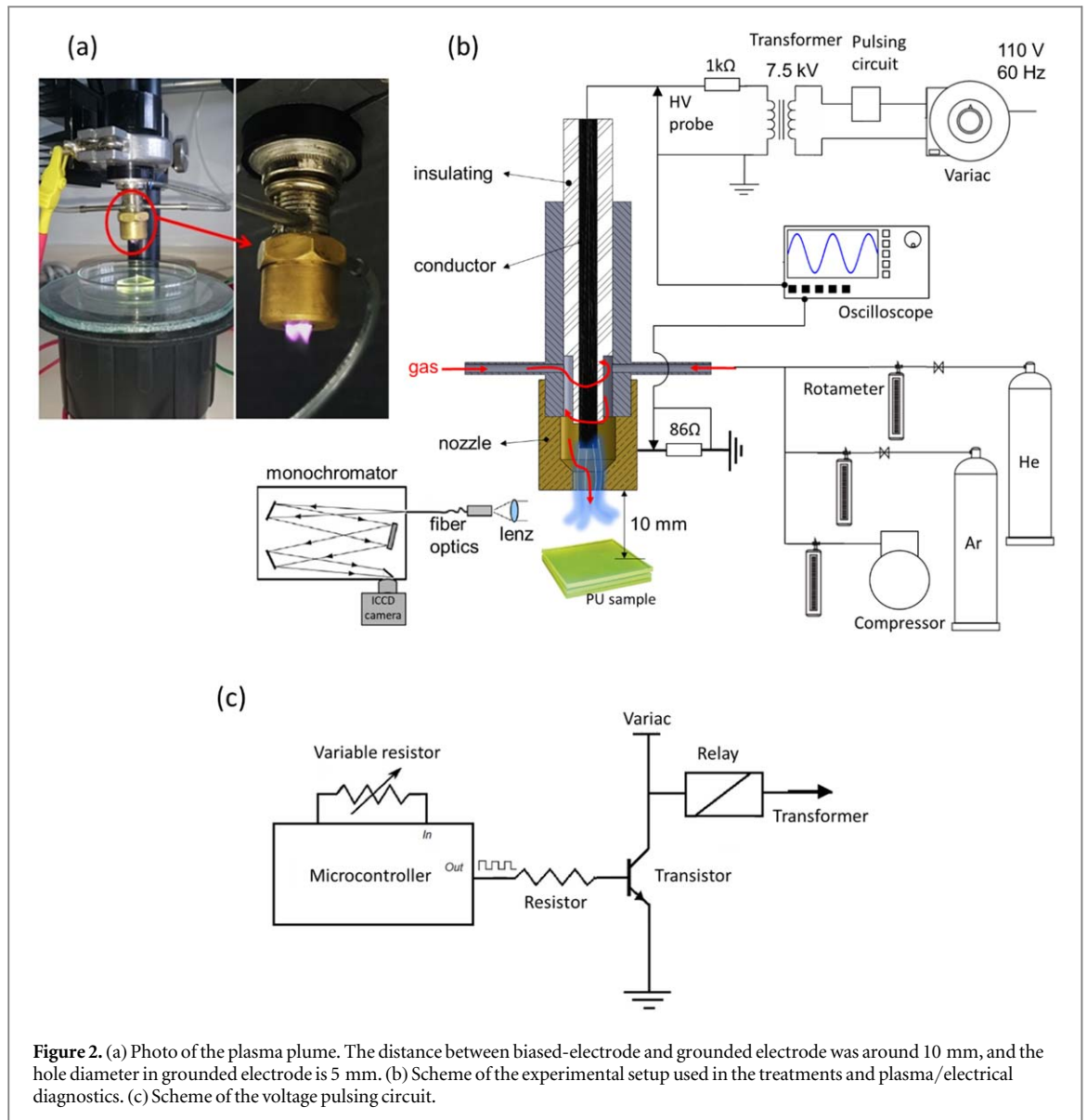


Figure 2. (a) Photo of the plasma plume. The distance between biased-electrode and grounded electrode was around 10 mm, and the hole diameter in grounded electrode is 5 mm. (b) Scheme of the experimental setup used in the treatments and plasma/electrical diagnostics. (c) Scheme of the voltage pulsing circuit.

Figure 3 shows the typical waveform for the voltage and current cycles. The discharge power is defined by

$$P(W) = \frac{1}{T_2 - T_1} \int_{T_1}^{T_2} V(t)I(t) dt \quad (1)$$

where $T_2 - T_1$ is the period (T), $V(t)$ the voltage (V) and $I(t)$ the current (A). Figure 4 illustrate the discharge power as a function of the fraction of gas flow. The discharge power varied between 15–25 W for all investigated air/Ar or air/He gas mixture conditions. For the case of pure argon and helium plasmas the discharge power was of 6.9 W and 9.8 W, respectively. These values were obtained for a fixed position of Variac transformer, i.e. the electrical parameters were influenced only by the gas mixture. A point to be highlighted from figure 3 is relative to the change of the waveform of the measured signals, especially for voltage. Zhang *et al* observed a similar effect using a GA system with pin-to-pin electrodes [23]. This condition of changing the waveform of the voltage, and also of the current, occurs when a nonstable discharge was obtained at a certain gap spacing in several seconds after the discharge went into a stable stage, whose appearance changed from a spark to a glow-like discharge [23]. Additionally, they emphasized that this discharge regime is highly dependent on the type of electric circuit used for plasma generation. The behavior of the waveform obtained in GA system used here will be better explored in a future work.

In addition, a homemade voltage pulsing circuit (figure 2(c)) was connected between the Variac and the high-voltage transformer to pulse the GA plasma. So, the difference between continuous mode and pulsed mode is related to the fact that in continuous mode the plasma is kept connected continuously throughout the treatment, whereas in pulse mode the plasma is pulsed at a frequency of 60 Hz by switching the electrical signal from the network to the transformer using the electric circuit shown in figure 2(c). This apparatus basically

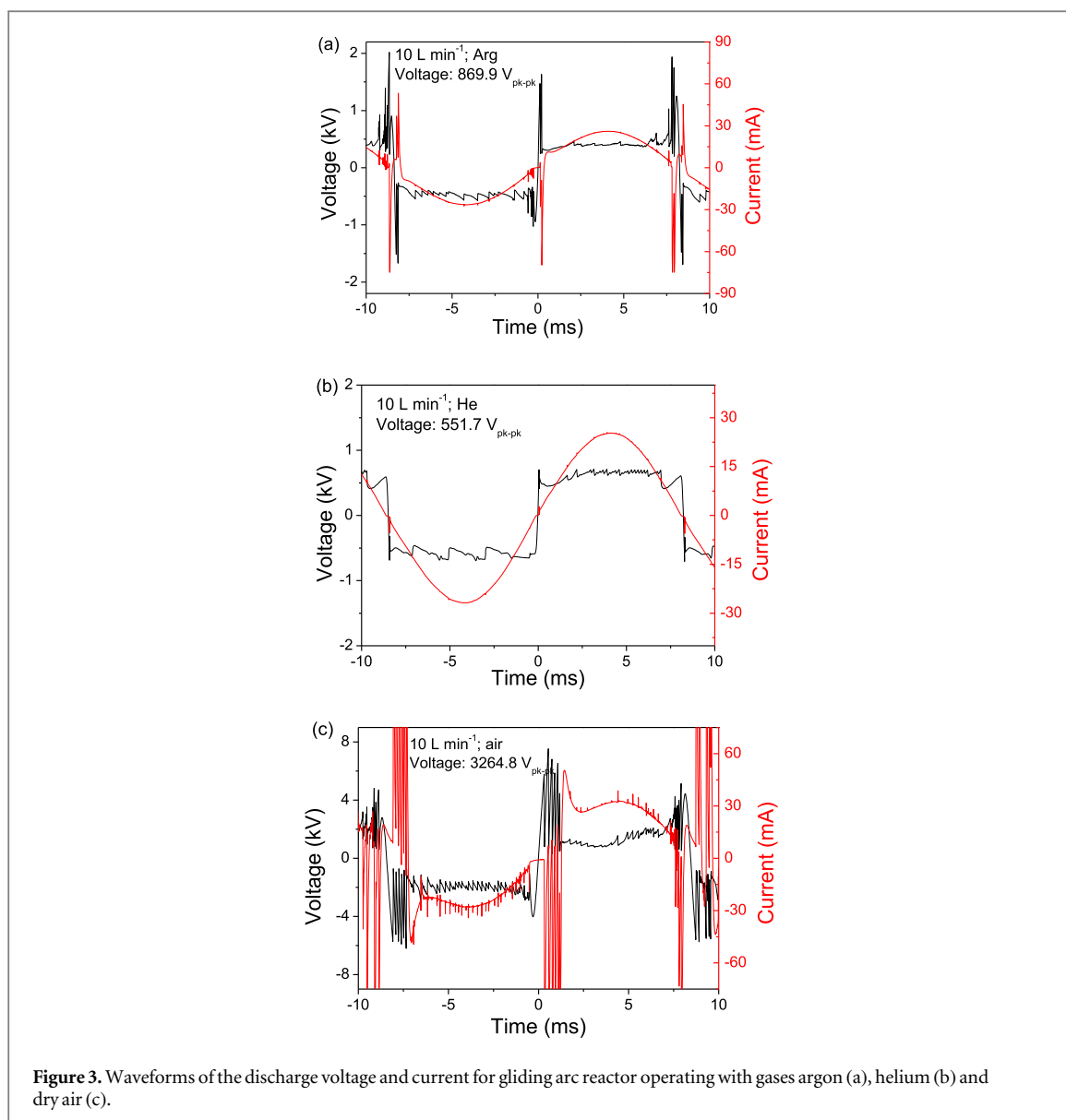


Figure 3. Waveforms of the discharge voltage and current for gliding arc reactor operating with gases argon (a), helium (b) and dry air (c).

reduces the exposure of the substrate to the plasma, because it is constantly being switched on and off along the treatment period. The purpose of the use of this apparatus was to reduce the heat caused by the continuous exposition of the PU substrate to the plasma effluent.

Optical emission spectroscopy (OES) was used to investigate plasma species in a UV-visible range of 200–500 nm. We used an Acton Spectra Pro SP-2500i monochromator with a Pixis 256 charge-coupled device camera (Princeton Instruments, Trenton, NJ), allowing a resolution of 0.05 nm. The optical spectrum was obtained through the Lightfield program, which allowed the determination of integration time to compose the spectrum, which was then displayed on a computer screen.

Finally, thermal imaging of the substrate surface during plasma treatment was done using an IR camera (model TiS 10, Fluke).

2.4. Experimental procedure and sample characterization

Treatments with GA plasma were performed immediately after washing the samples with PBS for a period of 10 min. Here, the sample holder was placed at 10 mm below the reactor, so the sample was treated in the post-discharge region because the plasma jet has a maximum length of 5 mm. All experiments were performed in triplicate and the samples were divided by the following plasma process parameters: gas flow/chemistry and plasma pulse mode, as presented in table 1.

After plasma application, the PU samples were placed in fresh tubes containing 10 ml of PBS and held for biofilm detachment using a vortex stirrer. Then 0.1 ml of this suspension was seeded on Sabouraud Dextrose agar by spreading technique and incubated at 37 °C for 48 h. The number of CFU/mL was counted using an electronic colony counter (Phoenix Luferto, Araraquara, SP, Brazil). The results were compiled for the

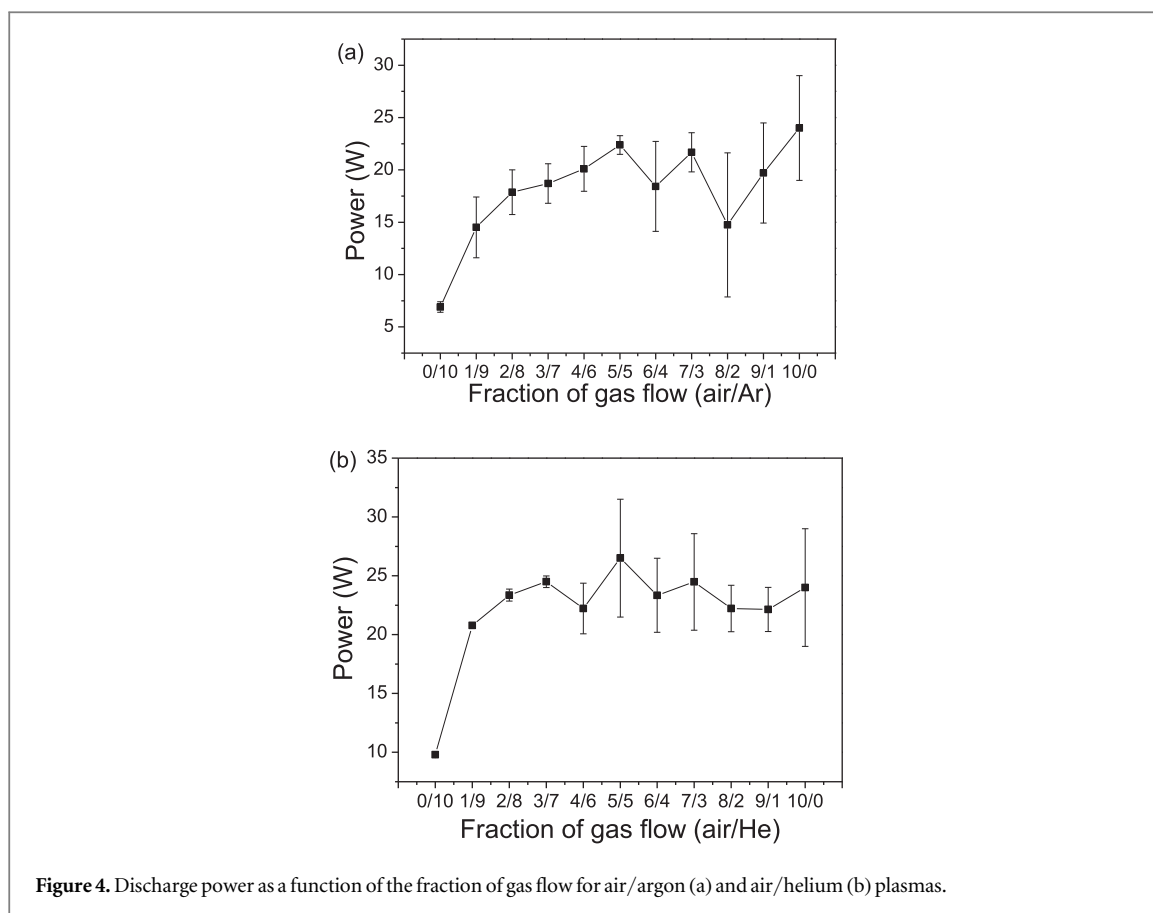


Table 1. Groups and respective plasma process parameters: gas flow/type and plasma pulse mode.

Group	Gas flow (L min ⁻¹)			Plasma pulse mode
	Argon	Helium	Air	
A	—	—	—	—
B1	6	—	4	Continuous
B2	—	6	4	Continuous
B3	—	10	—	Continuous
B4	10	—	—	Continuous
B5	—	1	9	Continuous
B6	1	—	9	Continuous
C1	6	—	4	Pulsed
C2	—	6	4	Pulsed
C3	—	10	—	Pulsed
C4	10	—	—	Pulsed
C5	—	1	9	Pulsed
C6	1	—	9	Pulsed

calculation of the colony reduction percentage using equation (2).

$$\% \text{ of reduction} = \frac{CFU \text{ count of control} - CFU \text{ count after treatment}}{CFU \text{ count of control}} \times 100. \quad (2)$$

We used the statistical inferential method to calculate the one-way analysis of variance (ANOVA), followed by application of a *post hoc* test (Tukey's multiple comparison test), to compare the treatment groups against the negative control. A level of 5% was considered significant ($p < 0.05$) [24].

The morphological modification of the treated *C. albicans* biofilm/PU substrate surface was analyzed by scanning electron microscopy (SEM) (model EVO MA 10; Zeiss, Oberkochen, Germany). To investigate the chemical bonds of biofilm/substrate, the infrared measurements were performed with attenuated total reflectance (ATR) Fourier transform infrared spectroscopy (FT-IR) on a 400 IR spectrometer (PerkinElmer,

Table 2. CFU/mL, percentage of reduction, p-value of the groups compared to the control population and mean temperature of the substrate during plasma treatment.

Group	CFU/mL	% of Reduction	T (°C) during treatment	p-value
A	1.798×10^4	—	—	—
B1	1.980×10^2	99%	39	1.221×10^{-08}
B2	3.800×10^1	100%	67	2.196×10^{-08}
B3	1.257×10^3	93%	32	1.440×10^{-08}
B4	5.290×10^2	97%	31	1.325×10^{-08}
B5	1.732×10^3	90%	49	1.541×10^{-08}
B6	1.367×10^3	92%	51	1.463×10^{-08}
Average B		95% (± 0.019)		
C1	4.220×10^2	98%	35	1.847×10^{-08}
C2	3.170×10^2	98%	35	3.694×10^{-08}
C3	9.090×10^2	95%	32	5.126×10^{-08}
C4	7.340×10^2	96%	29	4.538×10^{-08}
C5	1.774×10^3	90%	30	2.225×10^{-08}
C6	2.079×10^3	88%	32	2.160×10^{-07}
Average C		94% (± 0.020)		

Waltham, MA, USA) at a resolution of 2 cm^{-1} . Each FT-IR spectrum was recorded with the blank ATR cell as the background.

3. Results and discussion

3.1. Colony reduction

C. albicans biofilm inactivation experiments were carried out to observe the microbicidal efficacy of atmospheric GA plasma jet. The percentage of colony reduction is found to be dependent on various process parameters, such as gas chemistry/flow and gas pulse mode. The previous work [22] demonstrated the inactivation capacity of the GA plasma jet source in the biofilm of *C. albicans* and allowed us, in the present work, to optimize the process parameters in which the plasma efficacy is greater.

The CFU/mL before and after treatment with plasma are summarized in table 2. In addition, for comparison, the percentage of colony reduction obtained for each group, the p-value of ANOVA of each group with a significance level (α) of 5% and the mean surface temperature of the substrate during treatment are presented. Figure 5 shows a comparison of the CFU/mL between the control group A and the groups treated with different plasma process parameters. Each group is represented by its box plot showing the distribution of sampling results, including the minimum and maximum extremes.

In general, all treatment groups tested had a significant reduction of CFU. Groups B presented the mean reduction percentage of 95% ($\pm 0,019$) while groups C presented the mean of 94% ($\pm 0,02$). In figure 5, all groups maintained their dispersion close to zero. In addition to the counts shown in table 2, reductions up to 3 orders of magnitude in comparison to the control group were observed. Even though the results are positive, it is still possible to highlight Group B2 ($4 \text{ L min}^{-1} \text{ air} + 6 \text{ L min}^{-1} \text{ He}$, continuous mode) that presented the highest percentage reduction, 100% ($3,80 \times 10^1$ to $1,7980 \times 10^4$ CFU/mL), and the fourth quartile (upper limit 75% of the sample) is the closest to zero. It is believed that the relatively positive value using He was due to the combined action of the generation of OH species and the surface temperature achieved during treatment (about $64 \text{ }^\circ\text{C}$).

Through the box plot was possible to identify that the groups B1, B2, C1 and C2 presented better homogeneity in the reduction of microorganisms, which shows that the treatments are more likely to produce good results when applied on a larger scale. In relation to groups B5, B6, C5 and C6, it was possible to graphically observe a greater dispersion of the results, although they are statistically significant. The mean reduction in the CFU count of the treated groups was 95%, with only the groups B3, B5, B6, C5 and C6 achieving lower than average reductions. It is also observed that in these groups smaller proportions of noble gases were used in the gas mixture to generate the plasmas, a fact that influences the generation of reactive species, mainly OH, as discussed in topic 3.4.

Considering that the significance level (p) was set at 5%, it was found that all groups presented significantly different mean values in relation to control group A, indicating that the plasma treatments were effective in the control of biofilm contamination.

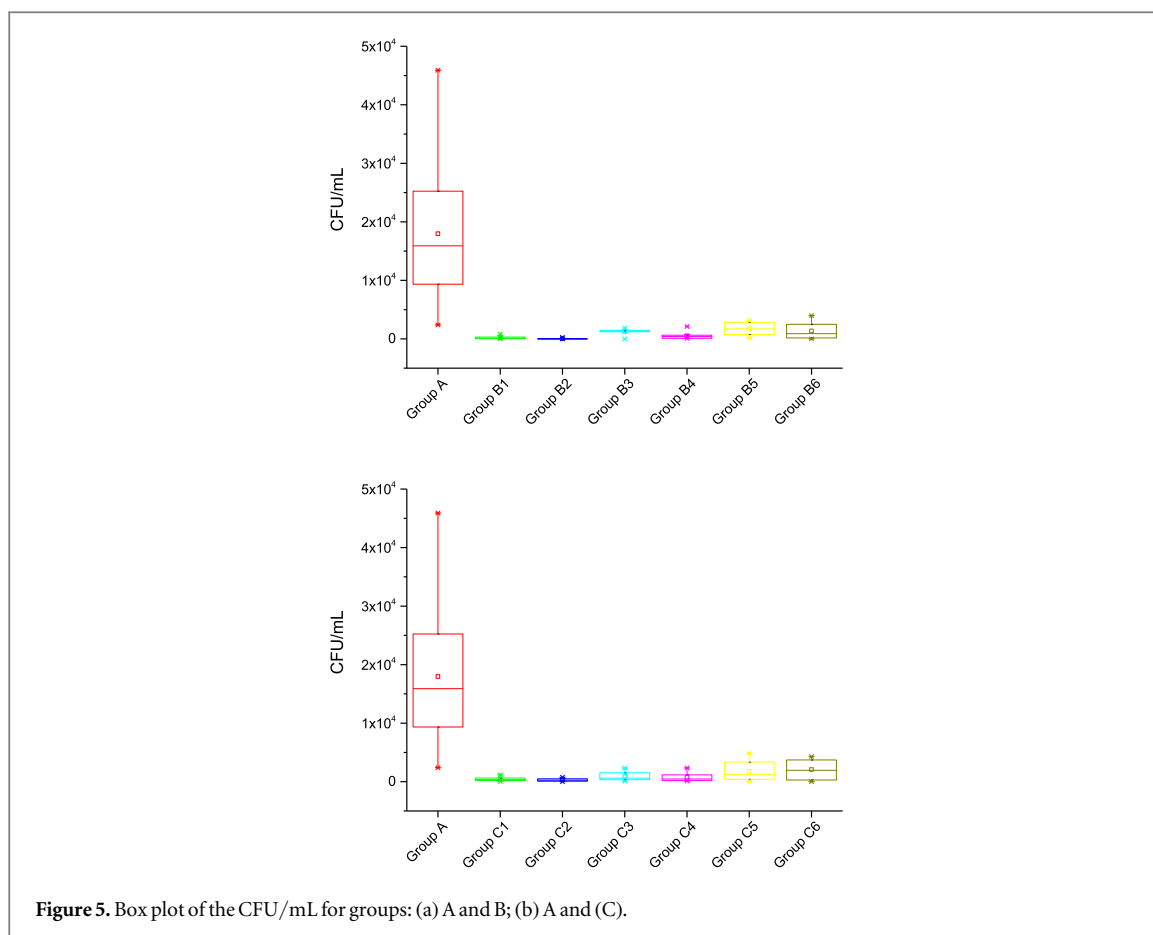


Figure 5. Box plot of the CFU/mL for groups: (a) A and B; (b) A and (C).

3.2. Surface morphology

After determining that we were able to reduce the colony number in the *C. albicans* biofilm by up to 90%–100% with a higher significance level, we performed SEM to visually observe the effects of plasma treatment on biofilm morphology.

Figure 6 shows SEM micrographs of the *C. albicans* biofilm on the PU surface for the control (positive and negative) and plasma-treated groups. One can observe from the positive control a dense biofilm that fills most of the area investigated. In fact, the biofilm growth period of 48 h and the surface roughness of the PU substrate allow a high adhesion of *C. albicans* cells and subsequent biofilm formation [6]. For plasma-treated biofilm/PU samples, SEM analyzes showed damaged cells, including hyphae, for all process parameters investigated. This possibly occurs due to oxidation, degradation or rupture of the cell wall. Cellular nonconformities may be related to the action of the hydroxyl radical on protein linkages in the outer cell membrane [25]. Consequently, extravasation of the cytoplasmic content to the extracellular medium occurs. Similar results of the morphology of plasma-treated *C. albicans* biofilm were obtained by Koban *et al* using the kINPen09 apparatus [24]. In addition, other works also observed biofilm remnants in the samples after plasma treatment [26, 27].

Comparing the different plasmas parameters used in our study, the antifungal efficacy of group B2 was significantly better than other conditions investigated. For this condition, a high reduction of the biofilm components present on the PU surface was observed. Groups B1 and C1–C5 also exhibited this behavior, although the respective % of colony reduction was lower than B2. The ‘flattening’ of the hyphae observed in some samples is believed to be a result of treatment with plasma.

3.3. Chemical bonds of non-treated and treated *C. albicans* biofilm/PU substrate

The FT-IR spectra resulting from the analysis of groups A, B and C are shown in figure 7. Figure 7(a) shows the spectra of the positive (biofilm + PU substrate) and negative (PU substrate) control groups. Figures 7(b) and (c) show the spectra of the treated material with plasma jet operated in continuous mode and different flow rate of He, Ar and its mixture with air. Figures 7(d) and (e) present the spectra of the treated material with plasma jet operated in pulsed mode in the same conditions of figures 7(b) and (c).

First, the typical bonds observed in PU substrate (negative group) were studied. The absorbance band at 3296.8 cm^{-1} is assigned to the N–H stretching vibrations. The peaks at 2940 and 2854 cm^{-1} can be attributed to

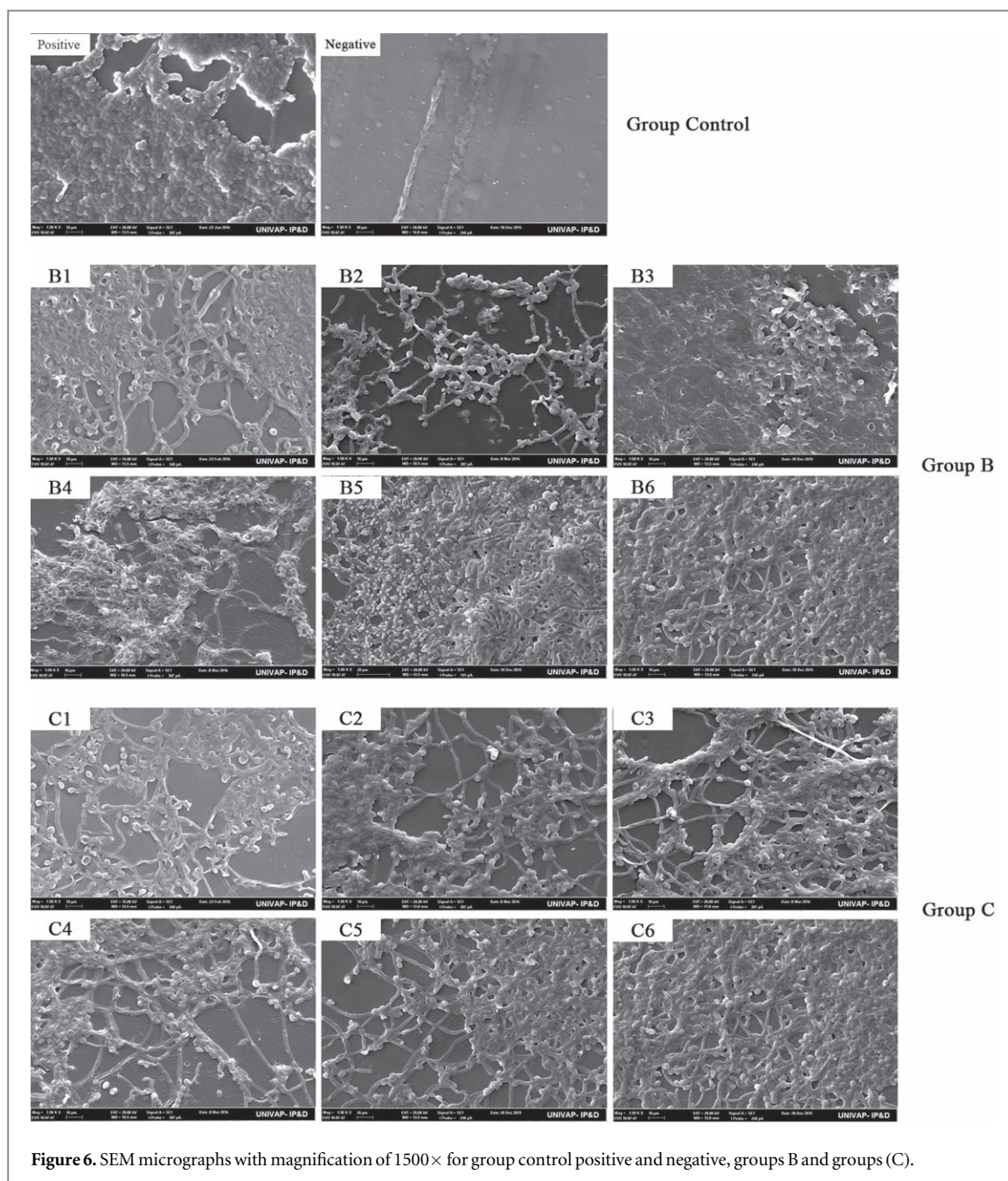


Figure 6. SEM micrographs with magnification of $1500\times$ for group control positive and negative, groups B and groups (C).

the asymmetric and symmetric stretching vibrations of CH_2 , respectively. The band at 1728 cm^{-1} is assigned to the stretching vibrations of hydrogen-bonded $\text{C}=\text{O}$ groups. The band at 1530 cm^{-1} is from amide II (urethane $\text{N}-\text{H}$ bending + $\text{C}-\text{N}$ stretching) and the bands at wavenumber of 1228 cm^{-1} and $\sim 1100\text{ cm}^{-1}$ are assigned to valence vibration of $\text{C}-\text{O}-\text{C}$ ($\text{C}-\text{O}$ single bond stretching modes) [6]. Secondly, the FT-IR spectrum of the biofilm + PU substrate (positive group) was analyzed. Note that bands related to the PU substrate are not identified, indicating the presence of a thick biofilm. As highlighted by Essendoubi *et al*, FT-IR spectroscopy is a whole-cell ‘fingerprinting’ method by which microorganisms can be identified [28]. The FT-IR spectrum of a biological system like *Candida* is relatively complex and consists of broad bands (see figure 7(a) that arise from the superposition of absorption peaks of various contributing macromolecules ($3200\text{--}3100\text{ cm}^{-1}$: NH from proteins; $2800\text{--}3000\text{ cm}^{-1}$: CH from lipids and proteins; $1720\text{--}1750\text{ cm}^{-1}$: $\text{C}=\text{O}$ from lipid esters; $1500\text{--}1700\text{ cm}^{-1}$: $\text{C}=\text{O}$ and $\text{N}-\text{H}$ from proteins; $1200\text{--}1250\text{ cm}^{-1}$: PO_2^- from nucleic acids, $900\text{--}1200\text{ cm}^{-1}$: various polysaccharide absorptions) [29].

After the plasma exposure, the bands related to PU appear together with the bands related to *C. albicans*. The intensity of each band shows to be dependent on the plasma condition used. For the condition of treatment with plasma operated in continuous mode, analyzing figure 7(b), it can be observed that the group B2 caused the highest reduction of the absorption bands relative to *Candida*. While from figure 7(c), it was found that groups

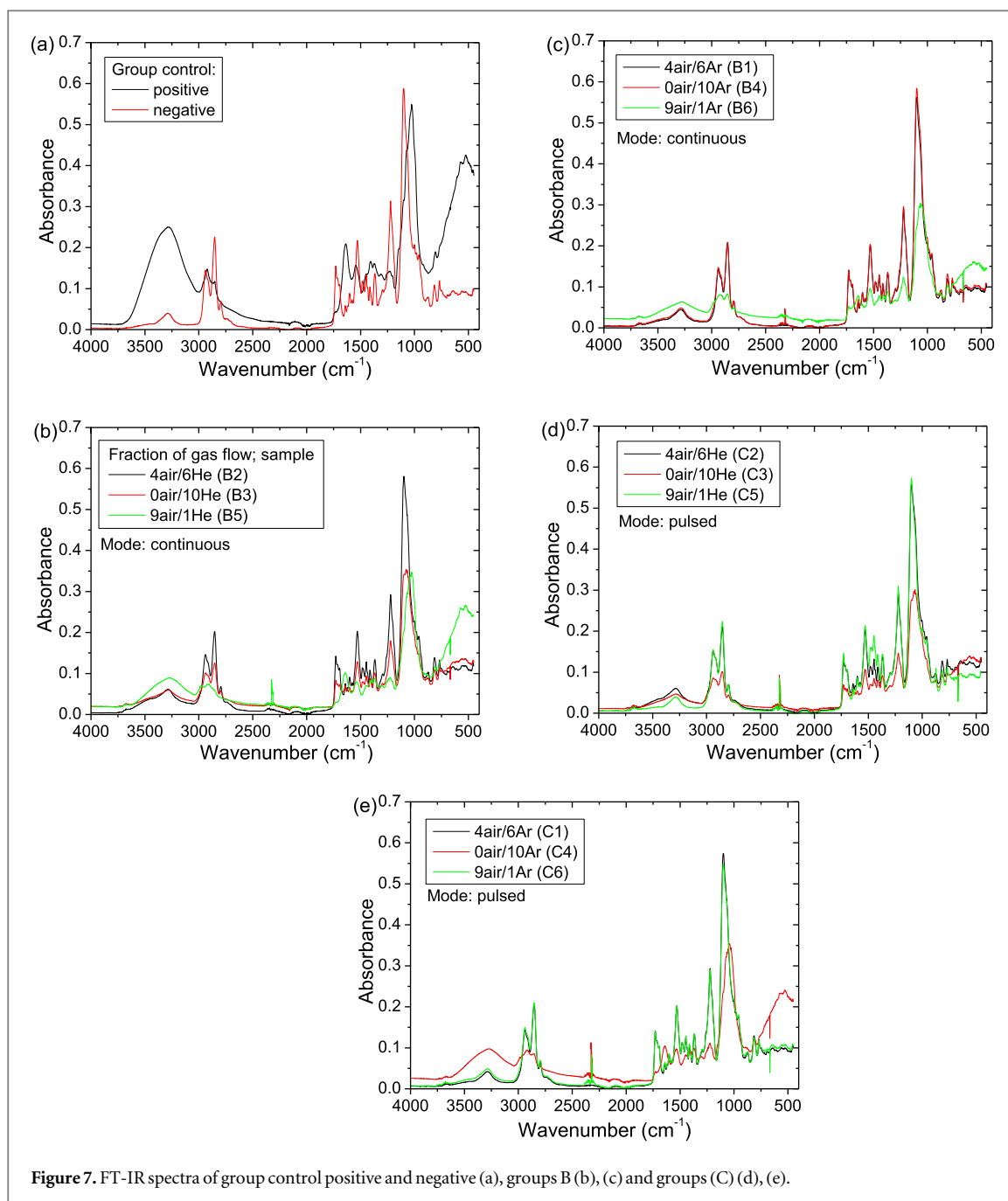


Figure 7. FT-IR spectra of group control positive and negative (a), groups B (b), (c) and groups C (d), (e).

B1 and B4 were equally effective. These results corroborate with SEM micrographs, which show a reduction of the biofilm on the substrate surface. A point to be highlighted from figures 7(b) and (c) is for groups B5 and B6, where 90% of air was used in the mixture with He and Ar, respectively. Note that under these conditions the bands relative to *Candida* are still evident, confirming the results of CFU reduction and SEM.

For the pulsed mode, groups C1, C2, C3, C5, C6 showed good reduction of the bands related to *Candida*. This result is interesting, since for group C4 was observed by SEM that a good part of the biofilm was decomposed by the action of the plasma, besides the biofilm reduction was very close to the group C6 and higher than the groups C3 and C5. Therefore, the FT-IR technique is an important complement for CFU analysis and may be used as an indicator of the inactivation of biofilm.

3.4. Optical emission spectroscopy of plasma jets and thermal analysis of the PU substrate

The last part of this study was the optical emission characterization of the GA plasma jets and thermal analysis of the contaminated PU substrate during plasma treatment.

OES was used to measure the optical emission of the plasma jets. Figures 8(a)–(c) show the emission spectra (200–500 nm) produced by the plasma jet of Ar and its mixture with air. As shown in the figure 8(a), the emission spectrum of the pure Ar plasma contains ArII states and NH, N₂ and a weak signal of the OH, that are coming

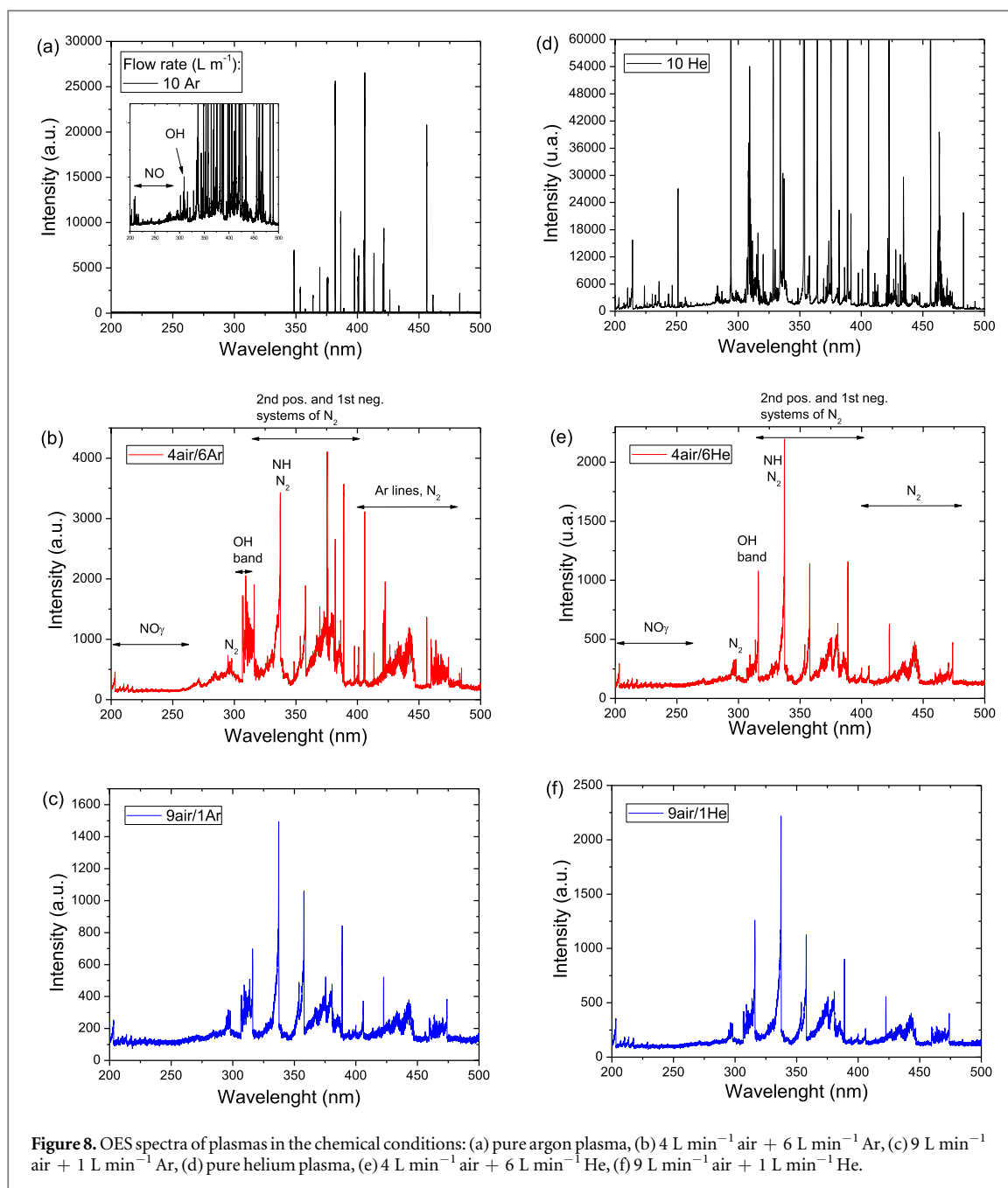


Figure 8. OES spectra of plasmas in the chemical conditions: (a) pure argon plasma, (b) 4 L min⁻¹ air + 6 L min⁻¹ Ar, (c) 9 L min⁻¹ air + 1 L min⁻¹ Ar, (d) pure helium plasma, (e) 4 L min⁻¹ air + 6 L min⁻¹ He, (f) 9 L min⁻¹ air + 1 L min⁻¹ He.

from mixing of Ar plasma with the surrounding air. With the addition and increase of dry air fraction (figures 8(b) and (c)), one can see that NO, OH, NH, N₂ and N₂⁺ are present in the air/Ar plasma plume. The emission bands of the NO_γ (A²Σ⁺ - X)-system at 200–280 nm were detected, but with low intensity [30]. The most intense emissions are observed between 300–500 nm, which are attributed to OH (A²Σ⁺ - X²Π_{3/2}) system, by argon atomic lines and by strong emissions from NH system (A³Π_u - X³Σ, 336 nm). Another prominent spectral feature is the second positive system (C³Π_u - B³Π_g) of N₂, especially the bands corresponding to the vibrational transitions 0–0 (band head at 336.9 nm), 1–0 (315.8 nm) and 0–1 (357.6 nm). Also, we can cite the first negative system (B²Σ_u⁺ - X²Σ_g⁺) of N₂⁺ at 389 nm. Also, in the region of 400 to 500 nm, generally are observed several lines of ArII that correspond to higher states of ionized argon [31]. The intensity of these spectral bands depends of the gas chemistry, in special, the amount of air mixed with noble gas.

In argon/nitrogen plasma, the population of the N₂ (C³Π_u) excited state may also result from the transfer of the internal energy from a metastable state of argon atoms to the ground state of the nitrogen molecules [32]. The metastable states of argon have the higher energies 11.55 and 11.72 eV than the threshold excitation energy (11.1 eV) of nitrogen molecule [32]. Therefore, by adding argon in air plasma a significant increase in the emission intensities and consequently the concentration of the active species can be expected by Penning effect [31, 32].

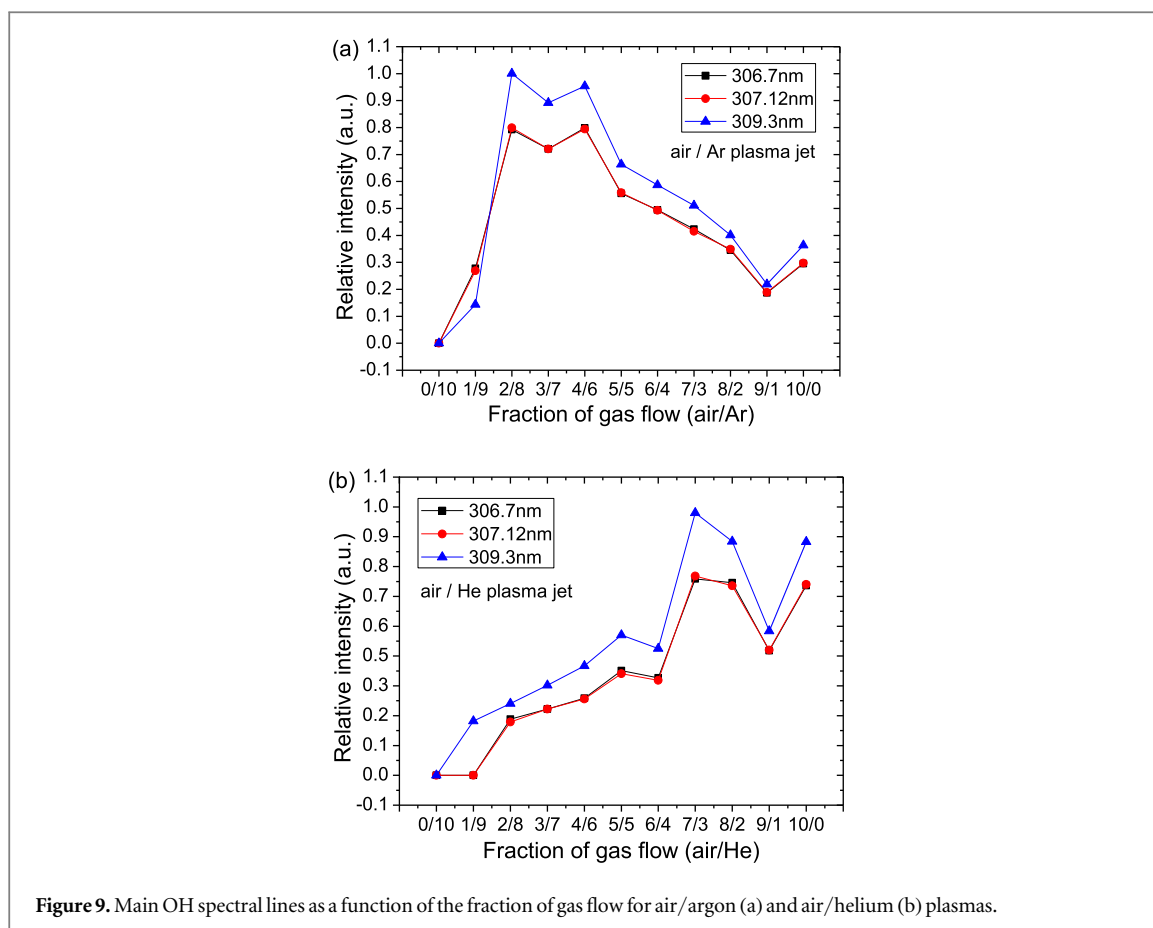


Figure 9. Main OH spectral lines as a function of the fraction of gas flow for air/argon (a) and air/helium (b) plasmas.

Figures 8(d)–(f) show the emission spectra produced by the plasma jet of He and its mixture with air. For pure He plasma jet, the length of the plume is around 1–2 mm, besides the light intensity is smaller as compared with the argon plasma. So, the emission spectrum was obtained for a longer integration time. The dominant emission lines illustrate the presence of the metastable helium atom, OH radical, NO radical and excited N_2 (figure 8(d)). With the addition of air, we can observe that the spectrum was totally dominated by air species, with a chemistry, in the range of 200–500 nm, very close to that observed for argon plus air plasma. The main difference can be observed in the intensities of the plasma species, especially for OH.

The main spectral lines of the OH radical ($\lambda = 306.7$ nm, 307.12 nm and 309.3 nm) as a function of Ar or He in air mixture are presented in figure 9. It can be observed from figure 9(a) that the highest OH intensity is between 2 and 4 $L \text{ min}^{-1}$ of air in the mixture with Ar, whereas for the He gas was around 7–10 $L \text{ min}^{-1}$. This result shows the great difference between the argon and helium gases when applied in atmospheric plasmas, showing that for practical applications the use of helium gas could be more interesting due to its low consumption. However, although it has a high OH concentration at higher content of air, when observed the results of figure 5 (samples B5 and B6 or C5 and C6), we can conclude that the argon gas allows a greater % reduction of CFU of *C. albicans*. This shows that other effects are occurring to cause inactivation of the microorganism. In fact, for samples B1 and B2 and C1 and C2, although the concentration of OH is higher in the range of gas flow investigated, the best inactivation condition was observed for He/air plasma.

The gas temperature is usually estimated from rotational temperature of some molecular species present in the plasma such as OH, N_2^+ or CN because of the highly favorable energy exchange between heavy particles and the internal rotational-vibrational states of the molecular species involved [33]. If admixture molecules are in equilibrium with most of the gas atoms, the rotational temperature (T_{rot}) derived from the ro-vibrational spectra can be considered equal to the gas temperature (T_{gas}). In this work, the T_{rot} was calculated using the intensities of particular selection of OH lines (see table 3 of [33]). Using the Boltzmann plot method [33] the T_{rot} of the plasmas generated in argon, helium and its mixture with air was determined. Although Zhao *et al* and Bruggeman *et al* evidenced that the rotational temperature from OH ($A^2\Sigma^+ - X^2\Pi_{3/2}$) was remarkably larger than that from N_2 ($C^3\Pi_u - B^3\Pi_g$) and N_2^+ ($B^2\Sigma_u^+ - X^2\Sigma_g^+$) [34, 35], the main idea of the calculation of the T_{rot} is to compare with the results of thermal analysis of substrate surface. Figure 10 shows the rotational temperature as a function of the fraction of gas flow for air/argon and air/helium. As can be seen, with the increase of the air flow rate in gas mixture, there is an increase of the T_{rot} and subsequent saturation for fraction of air/argon from 3/7

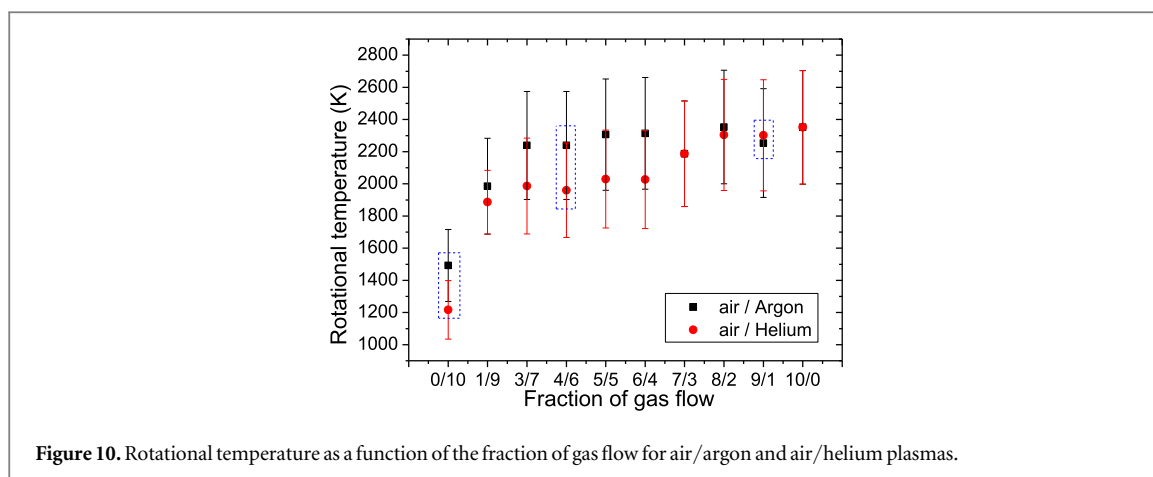


Figure 10. Rotational temperature as a function of the fraction of gas flow for air/argon and air/helium plasmas.

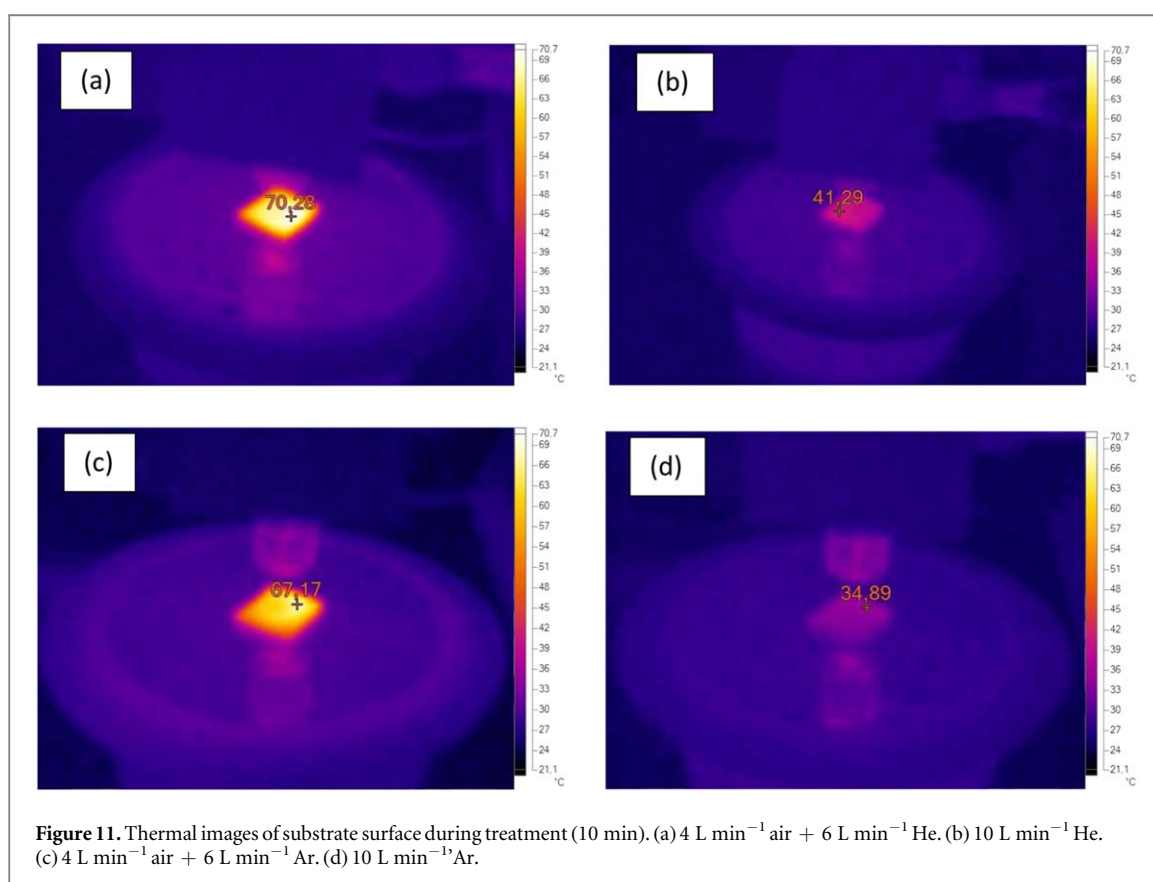


Figure 11. Thermal images of substrate surface during treatment (10 min). (a) 4 L min⁻¹ air + 6 L min⁻¹ He. (b) 10 L min⁻¹ He. (c) 4 L min⁻¹ air + 6 L min⁻¹ Ar. (d) 10 L min⁻¹ Ar.

(around 2300 K) and for air/helium from 8/2 (around 2350 K). Note that for a condition without air, the pure He plasma has a rotational temperature of the order of 1200 K. This temperature causes poor heating of the PU substrate (see figure 11(a)) and is therefore of interest for biological treatments. On the other hand, for a condition above 3 L min⁻¹ air, the gas rotational temperature was of the order of 2300 K, promoting a heating of up to 70 °C in the PU substrate during the treatment (figure 11(b)).

Comparing substrate temperature and % of CFU reduction data (table 2), we can observe a correlation between the results. However, the high substrate temperature observed for the 6 He/4 air condition does not show to be related to the rotational temperature as well as the OH concentration. Further studies are being carried out to explain this result.

Finally, through the thermal analysis of the substrate (figure 11), it was possible to verify that the pulsed mode of the plasma allowed a considerable decrease of the temperature of the substrate during the treatment period, maintaining the trend of the results obtained in the continuous mode.

4. Conclusion

In this work, we used an *in vitro* model to compare the efficacy of different plasma process parameters on inactivation of *C. albicans* biofilm grown on PU substrate. The plasma source used was a vortex GA plasma jet and the investigated parameters were: gas chemistry/flow and plasma operation in continuous or pulsed mode. The investigation was performed in post-discharge region using argon, helium and/or its mixture with air. CFU results showed that GA plasma jet was efficient for inactivation of *Candida albicans* biofilms. It obtained a maximum CFU reduction of 100% and 98% for air/He and 99% and 98% for air/Ar mixture in continuous and pulsed mode, respectively. SEM and FT-IR analyzes corroborate with results of % CFU reduction, showing a reduction of the biofilm constituents on the substrate surface. It is worth mentioning that the FT-IR technique may be used as an indicator of the inactivation of biofilm. From OES and substrate thermal analyzes, it was possible to verify that although the OH concentration and rotational temperature of air/He plasma jet is lower in comparison with air/Ar, a drastic increase of substrate temperature during treatment (up to 70 °C) was observed for this plasma chemistry. Further studies are being carried out to explain these last results. In general, the plasma equipment investigated herein was optimized for the treatment of PU substrates contaminated with *C. albicans* biofilm without damaging its integrity. For the case of treatment of polymers with greater thermal sensitivity or biological surfaces the pulsed mode can be used, but longer treatment periods will be required.

Acknowledgments

This work was supported by PROSUP-CAPES-Univap, CNPq-MCT/ FAPESP - PRONEX (grant No. 2011/50773-0), FAPESP (grants No. 2015/10876-6 and No. 2018/01265-1) and MCTI/CNPq/universal (grant No. 459688/2014-6).

ORCID iDs

R S Pessoa  <https://orcid.org/0000-0001-7600-9747>

References

- [1] Vargas-Blanco D, Lynn A, Rosch J, Noreldin R, Salerni A, Lambert C and Rao R P 2017 A pre-therapeutic coating for medical devices that prevents the attachment of *Candida albicans* *Ann. Clin. Microbiol. Antimicrobials* **16** 41
- [2] Colombo A L and Guimarães T 2003 Epidemiologia das infecções hematogênicas por *Candida spp* *Revista da Sociedade Brasileira de Medicina Tropical* **36** 599–607
- [3] Aguilar G, Delgado C, Corrales I, Izquierdo A, Gracia E, Moreno T and Belda F J 2015 Epidemiology of invasive candidiasis in a surgical intensive care unit: an observational study *BMC Res. Notes* **8** 491
- [4] Tan S Y-E, Chew S C, Tan S Y-Y, Givskov M and Yang L 2014 Emerging frontiers in detection and control of bacterial biofilms *Curr. Opin. Biotechnol.* **26** 1–6
- [5] Doria A, Figueira F, Lima J, Maciel H, Khouri S and Pessoa R 2016 Sterilization of *Candida Albicans* biofilms grown on polymers by atmospheric plasma: from plasma devices to biofilm analysis *Biofilms Characterization, Applications and Recent Advances* ed J Henderson (New York: Nova Science) pp 225–73
- [6] Pessoa R S et al 2017 TiO₂ coatings via atomic layer deposition on polyurethane and polydimethylsiloxane substrates: properties and effects on *C. albicans* growth and inactivation process *Appl. Surf. Sci.* **422** 73–84
- [7] Santos T B, Vieira A A, Paula L O, Santos E D, Radi P A, Khouri S, Naciel H S, Maciel H S, Pessoa R S and Vieira L 2017 Flexible camphor diamond-like carbon coating on polyurethane to prevent *Candida albicans* biofilm growth *J. Mech. Behav. Biomed. Mater.* **68** 239–46
- [8] Farrugia C, Cassar G, Valdramidis V and Camilleri J 2015 Effect of sterilization techniques prior to antimicrobial testing on physical properties of dental restorative materials *J. Dentistry* **43** 703–14
- [9] Arjunan K, Sharma V and Ptasinaka S 2015 Effects of atmospheric pressure plasmas on isolated and cellular DNA—a review *Int. J. Mol. Sci.* **16** 2971–3016
- [10] Moreau M, Feuilloley M G J, Orange N and Brisset J-L 2005 Lethal effect of the gliding arc discharges on *Erwinia spp* *J. Appl. Microbiol.* **98** 1039–46
- [11] Klämp T G, Isbary G, Shimizu T, Li Y-F, Zimmermann J L, Stolz W, Schlegel J, Morfill G E and Schmidt H 2012 Cold atmospheric air plasma sterilization against spores and other microorganisms of clinical interest *Appl. Environ. Microbiol.* **78** 5077–82
- [12] Winter J, Nishime T M C, Glitsch S, Lühder H and Weltmann K 2018 On the development of a deployable cold plasma endoscope *Contrib. Plasma Phys.* **58** 404–14
- [13] El-Aragi G M 2015 Inactivation of hepatitis C virus cells using gliding arc discharge *Plasma Medicine* **5** 49–55
- [14] Puligundla P and Mok C 2017 Potential applications of nonthermal plasmas against biofilm-associated micro-organisms *in vitro* *J. Appl. Microbiol.* **122** 1134–48
- [15] Fridman A, Nester S, Kennedy L A, Saveliev A and Mutaf-Yardimci O 1999 Gliding arc gas discharge *Prog. Energy Combust. Sci.* **25** 211–31
- [16] Kong M G, Kroesen G, Morfill G, Nosenko T, Shimizu T, van Dijk J and Zimmermann J L 2009 Plasma medicine: an introductory review *New J. Phys.* **11** 115012
- [17] Wang G M, Sun P P, Pan H, Ye G P, Sun K, Zhang J and Fang J 2016 Inactivation of *Candida albicans* biofilms on polymethyl methacrylate and enhancement of the drug susceptibility by cold Ar/O₂ plasma jet *Plasma Chem. Plasma Process.* **36** 383–96

- [18] Guofeng X and Xinwei D 2012 Electrical characterization of a reverse vortex gliding arc reactor in atmosphere *IEEE Trans. Plasma Sci.* **40** 3458–64
- [19] Rahimi-Verki N, Shapoorzadeh A, Razzaghi-Abyaneh M, Atyabi S-M, Shams-Ghahfarokhi M, Jahanshahi Z and Gholami-Shabani M 2016 Cold atmospheric plasma inhibits the growth of *Candida albicans* by affecting ergosterol biosynthesis and suppresses the fungal virulence factors *in vitro Photodiagn. Photodyn. Ther.* **13** 66–72
- [20] Borges A C, Nishime T M C, Kostov K G, Lima G M G, Gontijo A V L, de Carvalho J N M M, Honda R Y and Koga-Ito C Y 2017 Cold atmospheric pressure plasma jet modulates *Candida albicans* virulence traits. *Clinical Plasma Medicine* **7-8** 9–15
- [21] Simomura L, Doria A, Figueira F, Redi G, Lima J, Khouri S, Maciel H and Pessoa R 2017 Action of argon/water vapor plasma jet on *Candida albicans* biofilm grown on silicone substrate *Plasma Medicine* **7** 299–311
- [22] Doria A C O C, Sorge C, di P C, Santos T B, Brandão J, Gonçalves P A R, Maciel H S and Pessoa R S 2015 Application of post-discharge region of atmospheric pressure argon and air plasma jet in the contamination control of *Candida albicans* biofilms *Res. Biomed. Eng.* **31** 358–62
- [23] Zhang C, Shao T, Xu J, Ma H, Duan L, Ren C and Yan P 2012 A gliding discharge in open air sustained by high-voltage resonant AC power supply *IEEE Trans. Plasma Sci.* **40** 2843–9
- [24] Koban I et al 2010 Treatment of *Candida albicans* biofilms with low-temperature plasma induced by dielectric barrier discharge and atmospheric pressure plasma jet *New J. Phys.* **12** 73039
- [25] Khosravian N, Bogaerts A, Huygh S, Yusupov M and Neyts E C 2015 How do plasma-generated OH radicals react with biofilm components? Insights from atomic scale simulations *Biointerphases* **10** 29501
- [26] Matthes R, Bender C, Schlüter R, Koban I, Bussiahn R, Reuter S, Lademann J, Weltmann K-D and Kramer A 2013 Antimicrobial efficacy of two surface barrier discharges with air plasma against *in vitro* biofilms *PLoS ONE* **8** e70462
- [27] Rupf S et al 2011 Removing biofilms from microstructured titanium *ex vivo*: a novel approach using atmospheric plasma technology *PLoS ONE* **6** e25893
- [28] Essendoubi M, Toubas D, Bouzaggou M, Pinon J-M, Manfait M and Sockalingum G D 2005 Rapid identification of *Candida* species by FT-IR microspectroscopy *Biochimica et Biophysica Acta* **1724** 239–347
- [29] Toubas D, Essendoubi M, Adt I, Pinon J-M, Manfait M and Sockalingum G D 2007 FTIR spectroscopy in medical mycology: applications to the differentiation and typing of *Candida* *Anal. Bioanal. Chem.* **387** 1729–37
- [30] Moisan M et al 2013 Sterilization/disinfection of medical devices using plasma: the flowing afterglow of the reduced-pressure N₂-O₂ discharge as the inactivating medium *Eur. Phys. J. Appl. Phys.* **63** 10001
- [31] Pessoa R S, Sismanoglu B N, Gomes M P, Medeiros H S, Sagás J C, Roberto M, Maciel H S and Petraconi G 2013 Chemistry studies of low pressure argon discharges: experiments and simulation *Argon: Production, Characteristics and Applications* (New York: Nova Science)
- [32] Qayyum A, Zeb S, Naveed M A, Rehman N U, Ghauri S A and Zakaullah M 2007 Optical emission spectroscopy of Ar-N₂ mixture plasma *J. Quant. Spectrosc. Radiat. Transfer* **107** 361–71
- [33] Hnilica J, Potočnáková L and Kudrle V 2015 Time resolved optical emission spectroscopy in power modulated atmospheric pressure plasma jet *Open Chem.* **13** 577–85
- [34] Zhao T, Xu Y, Song Y, Li X, Liu J, Liu J and Zhu A 2013 Determination of vibrational and rotational temperatures in a gliding arc discharge by using overlapped molecular emission spectra *J. Phys. D: Appl. Phys.* **46** 345201
- [35] Bruggeman P J, Sadeghi N, Schram D C and Lins V 2014 Gas temperature determination from rotational lines in non-equilibrium plasmas: a review *Plasma Sources Sci. Technol.* **23** 023001–21